

THE SELF-ASSEMBLING PEPTIDE RADA16-I SUPPRESSES THE MALIGNANT PHENOTYPE OF PANCREATIC CANCER CELL LINE MIAPaCa-2 IN THREE-DIMENSIONAL CULTURE AND *IN VIVO*

ZHANG WEN, YA HU^a, QUAN LIAO, YUPEI ZHAO*

Department of General Surgery, Peking Union Medical College Hospital, Chinese Academy of Medical Sciences and Peking Union Medical College, Tsinghua University, Beijing 100730, China.

Malignancy is a state that emerges from a tumour-host microenvironment in which the host participates in inducing, selecting, and expanding tumour cells. The tumour environment modifies the malignant phenotype of the tumour cells, including morphology, survival, proliferation, and invasion. In this study, we investigated effects of the self-assembling peptide RADA16-I, compared with Matrigel and Collagen I, on the malignant phenotype of a pancreatic cancer cell line, MIAPaCa-2, in three-dimensional culture and *in vivo*. We showed that MIAPaCa-2 cells adjusted their malignant phenotype in these differing extracellular matrices. RADA16-I creates a nanoscale matrix, without animal-derived materials, and can greatly suppress the malignant phenotype of MIAPaCa-2 cells in three-dimensional culture and *in vivo*. These results suggest that the self-assembling peptide RADA16-I is a potential nanomaterial for pancreatic cancer research and treatment.

(Received November 9, 2012; Accepted January 28, 2013)

Keywords: Self-assembling peptide; RADA16-I; Pancreatic cancer cell line; three-dimensional culture

1. Introduction

The tumour microenvironment has been widely accepted as playing a crucial role in cancer initiation and progression, containing vessels and lymphatic ducts, a neuronal network and immune/inflammatory cells in an extracellular matrix (ECM)[1, 2]. Most tumours cannot survive without tumour microenvironment support[3]. Studies of the tumour microenvironment could improve our understanding of tumours and provide novel strategies for diagnosis and treatment.

Pancreatic cancer is the most lethal malignant disease and has a poor prognosis, largely due to aggressive growth and early metastases. A typical property of pancreatic cancer is its prominent desmoplastic reaction. There is increasing recognition of the crucial role played by the pancreatic cancer microenvironment in tumour initiation and distant spread[4, 5]. Thus, the interaction of pancreatic cancer cells and the tumour microenvironment should be intensely evaluated, in both basic and clinical research into pancreatic cancer[6, 7].

Studies of oncology, based on traditional two-dimensional (2D) cultures, have helped us to understand many aspects of cancer. However, 2D cultures cannot comprehensively mimic morphology, cell-to-cell and tumour-environment interactions *in vivo*. There is increasing recognition that three-dimensional (3D) culture, which recaptures the phenotype and genotype of

* Corresponding author: zhao8028@263.net

tumour *in vivo*, is a promising model for studying cancer biology and developing novel treatments[8, 9].

The most common used ECMs for 3D culture are animal-derived materials, such as Matrigel and Collagen I but their compositions are complex and the materials are undefined, so their applications are limited[10]. Recent studies have also revealed that self-assembling peptides used in 3D cultures have shown promising potential in various fields, such as membrane protein stabilizers[11], drug delivery vehicles[11, 12], hemostasis agents[13], scaffolds for cell culture and tissue engineering[14, 15], cell sheet technology[16], and regenerative medicine[17]. Self-assembling peptides could create a novel class of nanoscale biomaterials. Furthermore, these peptides do not contain animal-derived materials, are facilitatively controlled, and do not induce immune responses[18].

In the present study, we compared, for the first time, the effects of the self-assembling nanofiber peptide RADA16-I with those of Matrigel and Collagen I on a human pancreatic cancer cell line, MIAPaCa-2. We identified the malignant phenotype, including the morphology, proliferation and invasive potential, and the effects of these ECMs on MIAPaCa-2 *in vivo*.

2. Experimental section

2.1 Materials

PuraMatrix: RADA16-I ([COCH₃]-RADARADARADARADA-[CONH₂]) solution (1%) was purchased from BD Bioscience (Bedford, MA, USA). PuraMatrix was sonicated for 30 min before cell culture. Matrigel and Collagen I were purchased from BD Bioscience. Calcein AM, Tubulin Tracker Green reagent for live-cell tubulin labelling (Oregon Green 488 Taxol, bis-acetate, T34075), and 4',6-diamindino-2-phenylindole (DAPI) were purchased from Molecular Probes (Eugene, USA). A DNA Quantitation Kit and rhodamine phalloidin were purchased from Sigma (St. Louis, MO, USA). The Click-iT EdU HCS assay was purchased from Invitrogen (Carlsbad, California, USA). Dulbecco's Modified Eagle's Medium/high glucose medium, fetal bovine serum (FBS), phosphate buffered saline (PBS) and penicillin/streptomycin were purchased from HyClone (Logan, UT, USA).

2.2 Structural studies

Stock solutions of RADA16-I, Matrigel, and Collagen I were diluted with 0.01 M PBS to concentrations of 0.1, 0.06, and 0.05 mg/ml, respectively. Working solution was negatively stained with 1% uranyl acetate and placed on a transmission electron microscopy (TEM) copper grid, covered by a perforated poly(vinyl formal) film. After drying, TEM images were analyzed by observing the TEM grid on a JEM-100 electron microscope (JEOL Ltd., Tokyo, Japan)[14].

2.3 Cell culture

The MIAPaCa-2 human pancreatic cancer cell line was gifted by Professor Friess at the Department of Surgery, Technische Universitt, München, Germany. The cell line was cultured in DMEM/high glucose medium supplemented with 10% FBS and 1× penicillin/streptomycin. Cancer cells were cultured in the 3D system according to the protocols for a different matrix. Briefly, cells cultured in a monolayer were trypsinized, washed and pelleted, and in the RADA16-I peptide 3D culture, cells were suspended in 10% sucrose solution. After mixing the cell suspension and RADA16-I at a ratio of 1:1, the mixture was placed into the culture well and the well was then filled with medium. The peptide was allowed to self-assemble for 30 min and then half of the culture medium was changed until a pH of 7.4 was reached. The medium was changed every 2 days[19]. Cells were cultured in a 1:1 dilution of Matrigel with a concentration of 5 mg/ml[20]. Collagen I was prepared at a concentration of 1.5 mg/ml[21]. The cancer cells were cultured in an 8-well-culture plate. The number of cells was equal at the beginning of embedding in the different ECMs. After 30 min incubation at 37 °C, the gels were covered with complete culture medium, which was changed at 2-day intervals. A LEICA DMIL phase-contrast microscope (Leica, Wetzlar, Germany) was used for routine observation.

2.4 DNA-content measurement

The density of cells in the different ECMs was evaluated by cellular DNA, analyzed by fluorometric quantification. The 3D cultures were washed with PBS, placed in 50×10^{-3} M sodium citrate buffer solution, and stored at -80 °C. After thawing, the cells were lysed with sodium citrate solution. 10 μ M of the cell lysate was mixed with the assay buffer and fluorescent dye. The fluorescent intensity was measured by a fluorescence spectrometer. The calibration relationship between cell density and DNA was evaluated over a range of cell densities[22].

2.5 Immunostaining

The 3D culture was fixed with 4% polyoxymethylene for 10 mins. For immunostaining, the culture was blocked by the immunofluorescence buffer containing 10% goat serum[23]. Calcein AM working solution (2×10^{-6} M) was diluted with PBS to investigate living MIAPaCa-2 cells. Tubulin Tracker Green reagent for live-cell tubulin labeling (125 nM), rhodamine phalloidin working solution (5 U/ml), and DAPI working solution (300 nM) were diluted with PBS for tubulin, F-actin, and nuclei staining, respectively. The images were analyzed by an UltraVIEW VoX-3D live cell imaging system (Waltham, MA, USA).

2.6 EdU Assay

The Click-iT EdU HCS assay was used to detect and quantify newly synthesized DNA. The cultures of MIAPaCa-2 cells were prepared following the above methods. The assay steps were performed according to the supplier's instructions. Briefly, cells in 3D culture were fixed with 3.7% formaldehyde in PBS for 15 min. Cell permeabilization was attained by adding 0.1% Triton X-100 in PBS to the well and incubating for 15 min. After the wash solution was removed, the Click-iT reaction cocktail was added and incubated for 30 mins. Samples were rinsed with the Click-iT reaction rinse buffer. Nuclei staining was carried out using $1 \times$ HCS Nuclear Mask Blue stain solution for 30 min. EdU-labeled nuclei were scored using 200 cells per experiment and the indices were expressed by the percentage of the labeled nuclei[24].

2.7 Invasive assay

Briefly, MIAPaCa-2 cells were serum-deprived for 24 h. Subsequently, 2.0×10^4 cells were seeded in the upper chamber as 3D cultures, using an 8 μ m transwell membrane. The lower chamber contained medium with 5% FBS as a chemoattractant. The cells were incubated for 48 h. The inserts were then fixed with methanol and stained with DAPI. The cells on the lower surface of the membrane were counted in 5 random fields at $\times 200$ magnification.

2.8 In vivo experiments

MIA PaCa-2 cells were cultured in a monolayer, then trypsinized, centrifuged and resuspended, and mixed with Matrigel, Collagen I, and RADA16-I (final concentrations of 5, 1.5, and 5 mg/ml, respectively). Subsequently, 3×10^6 cells were subcutaneously injected into the axillary mammary fat pads of 4- to 6-week-old BALB/c nude mice. MIAPaCa-2 cells, alone, were injected as negative controls. Eight mice were used in each group. After forty days of transplantation, the tumours were harvested. The volume of each tumour was calculated as follows: $\pi/6 \times (L \times W \times W)$, where L is the largest and W the smallest diameter of the tumour, respectively. Animal procedures complied with the guide for the care and use of laboratory animals[25].

2.9 Statistical analysis

Statistics analysis was performed using the one-way ANOVA test, and differences were judged to be significant at $P < 0.05$.

3. Results

3.1 Structure of RADA16-I, Matrigel, and Collagen I

TEM was applied to evaluate nanofiber formation. It has been shown that RADA16-I transforms to a β -strand structure, self-assembles into nanofibers and finally a hydrogel scaffold [26]. Similar nanofibers were also observed in RADA16-I after self-assembly in PBS. TEM images of RADA16-I, Matrigel, and Collagen I are shown in Figure 1.

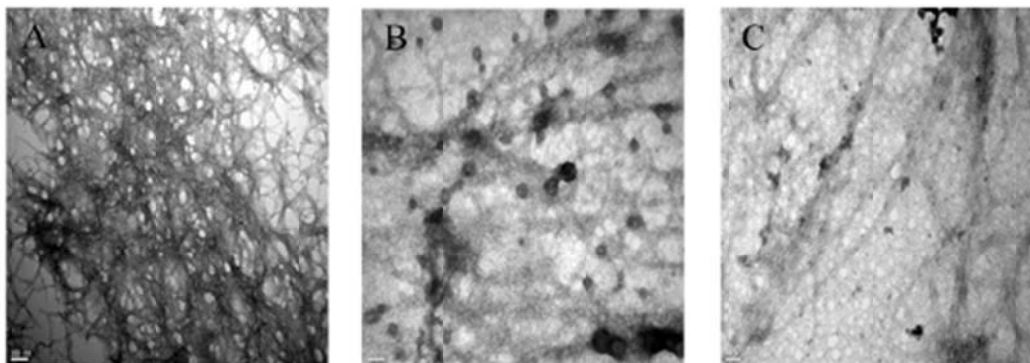


Fig. 1. TEM images of (A) RADA16-I peptide nanofiber matrices, (B) Matrigel, and (C) Collagen I (Bar: 100 nm)

3.2 The morphology of the MIAPaCa-2 cells in 3D culture in different ECM

To investigate MIAPaCa-2 cell distribution and viability in the 3D culture in three different ECMs, MIAPaCa-2 cells were cultured for 3 days and stained with calcein AM. The viabilities of MIAPaCa-2 cells cultured in the three ECMs were good (Figure 2). The cells in Collagen I showed a myofibroblast form, while, in contrast, the cells in RADA16-I and Matrigel maintained a spheroid form during 3D culture.

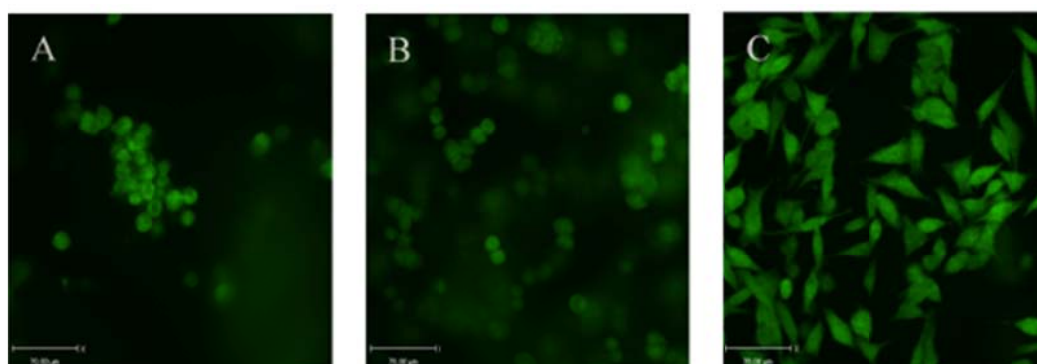


Fig. 2. Three-dimensional culture of MIA PaCa-2 cells in (A) RADA16-I, (B) Matrigel, and (C) Collagen I using calcein AM staining for living cancer cells for 3 days. MIA PaCa-2 cells showed myofibroblast-like shapes in Collagen I, while the cells maintained a multicellular spheroid form in RADA16-I and Matrigel. (Bar: 70 μ m)

To investigate the 3D morphologies of MIAPaCa-2 cells in the different ECMs, the cells were observed on the localization of F-actin and tubulin after 5 days (Figure 3). Cells grown in RADA16-I and Matrigel showed the shape of multicellular spheroids. However, cells in the

Collagen I 3D culture showed a myofibroblast-like shape, which indicates a mesenchymal phenotype.

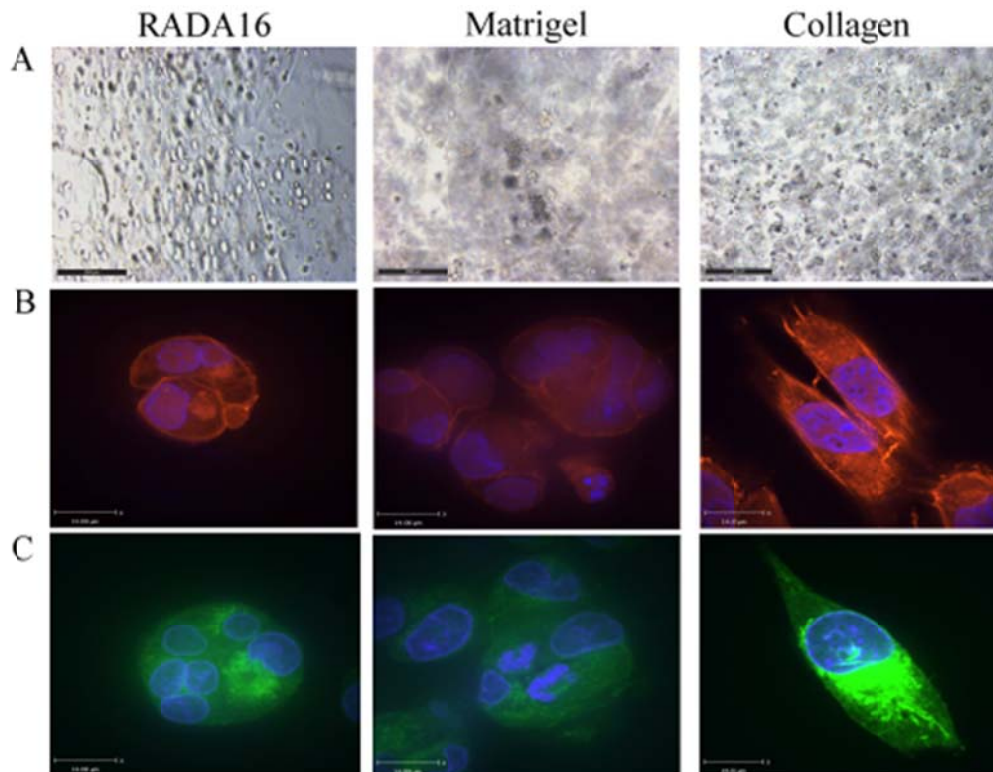


Fig. 3. Differing morphologies of MIA PaCa-2 cells in different ECMs: (A) light microscopy images of cells in RADA16-I, Matrigel, and Collagen I for 3 days. (B) F-actin cytoskeleton (red) and nuclear (blue) fluorescence images of morphology in RADA16-I, Matrigel, and Collagen I. (C) Tubulin (green) and nuclear (blue) fluorescence images of morphology in RADA16-I, Matrigel, and Collagen I. (Bar in row A: 200 μm . Bar in rows B and C: 14 μm)

3.3 The proliferation of MIA PaCa-2 cells in different ECM

MIAPaCa-2 cells cultured in the RADA16-I, Matrigel, and Collagen I ECMs were investigated for proliferation by measuring DNA content (Figure 4A). In Matrigel and Collagen I, the cell density increased during the period of culture and the cell density in Matrigel was the highest. On the other hand, the cell density in the RADA16-I increased before day 5 but did not significantly increase thereafter.

Correspondingly, the percentage of EdU labelling in MIAPaCa-2 cells in the three ECMs was expressed as the EdU labelling indices at days 3, 5, and 7 (Figure 4B). Our study shows that approximately 89% of the MIAPaCa-2 cells in RADA16-I stopped proliferating on day 7. Thus, the results of incorporating EdU into the DNA matched the results of DNA content measurements of MIAPaCa-2 cells in different ECMs.

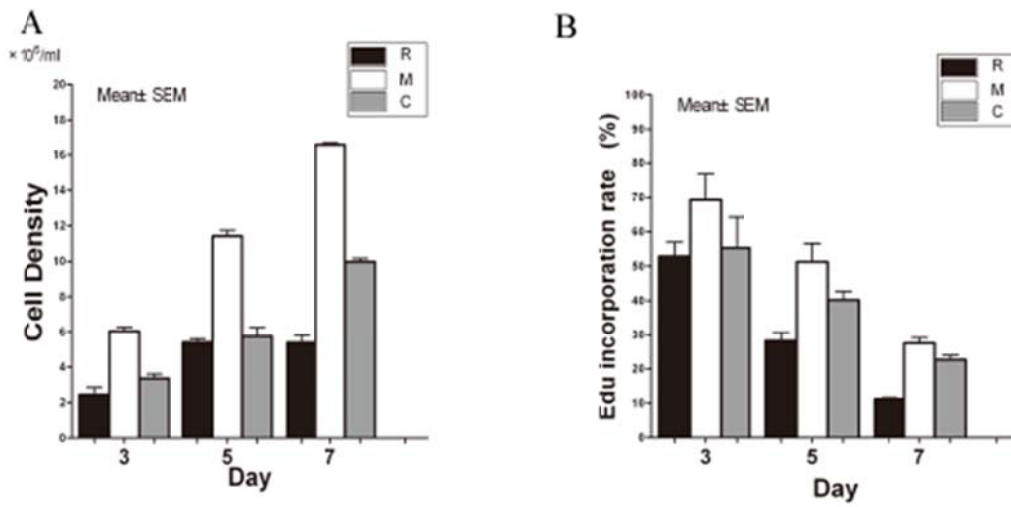


Fig. 4. The proliferation of MIAPaCa-2 cells in 3D culture with different ECMs. (A) MIAPaCa-2 cell density in different ECMs evaluated by DNA measurements after 3, 5, and 7 days of culture. (B) The percentage of EdU labelling in MIA PaCa cells grown in different matrices, expressed as the EdU labelling index at days 3, 5, and 7.

3.4 The invasive potential of MIA PaCa-2 cells in different ECM

To investigate the invasive potential of MIAPaCa-2 cells in different ECMs, the cells were analyzed with transwell chamber assays (Figure 5). Compared with MIAPaCa-2 cells in Collagen I, 52.60% of the cells in Matrigel and 3.44% of the cells in RADA16-I invaded through the matrix. Significant differences were observed between the three groups ($p < 0.001$).

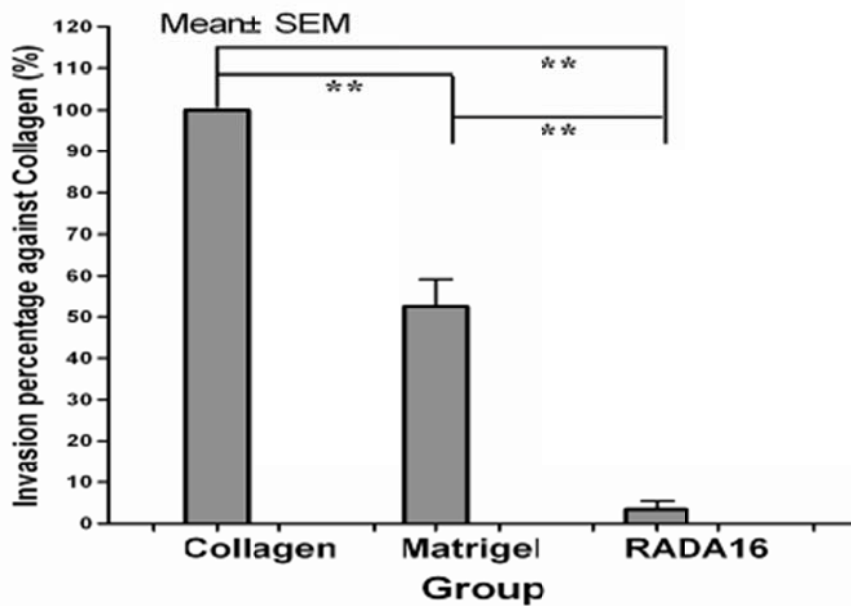


Fig. 5. Invasion of MIAPaCa-2 cells in Collagen I, Matrigel, and RADA16-I. Each column represents an invasion percentage against Collagen I (%). ** $P < 0.001$

3.5 Tumour growth in vivo

To evaluate the effects of different ECMs on tumour growth *in vivo*, we transplanted MIAPaCa-2 cells with RADA16-I, Matrigel, and Collagen I into nude mice, while MIAPaCa-2 cells alone were transplanted (the 2D group) as a control group. Forty days after implantation, we observed that adding Matrigel and Collagen I prominently enhanced the weight and volume of the tumours, compared with the RADA16-I group ($P < 0.001$) (Figure 6A, B and C).

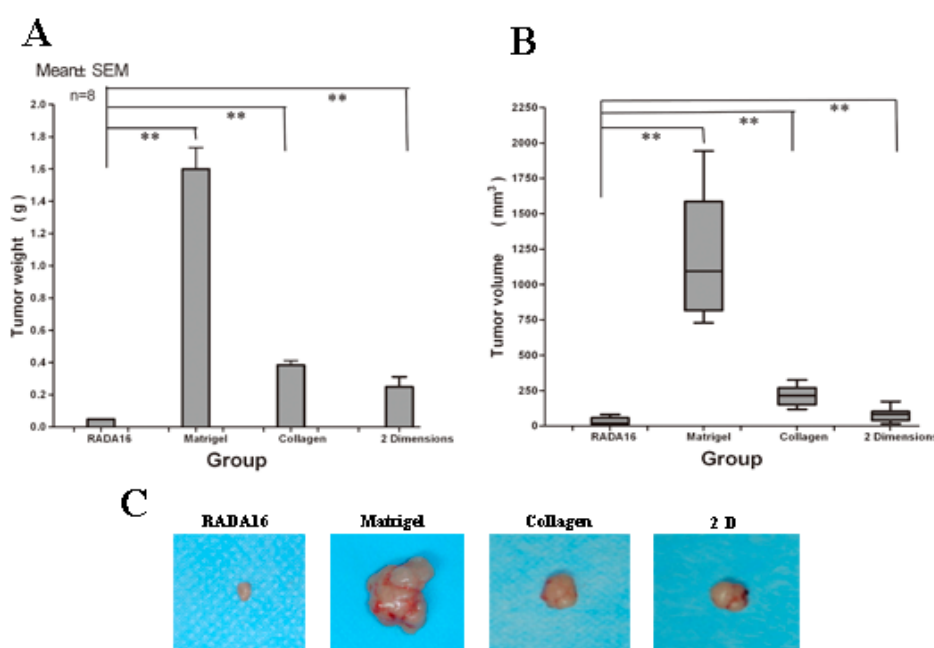


Fig. 6. (A) Effects of RADA16-I, Matrigel, and Collagen I on the tumor weight of MIAPaCa-2 cells. RADA16-I significantly reduced the tumour weight compared with other groups (** $P < 0.001$). (B) Effects of RADA16-I, Matrigel, and Collagen I on the tumour volume of MIAPaCa-2 cells. RADA16-I significantly reduced the tumor volume compared with other groups (** $P < 0.001$). (C) Tumours formatted in RADA16-I, Matrigel, Collagen I and 2D culture. Eight mice were used in each group.

4. Discussion

Although traditional 2D culture has contributed greatly to pancreatic cancer research, it has limitations that have promoted the development of 3D culture. 3D culture can mimic the interactions between tumour and the surrounding microenvironment *in vivo*. Several studies have investigated pancreatic cancer cells in 3D culture using animal-derived materials [27, 28]. The resultant malignant phenotype is remarkably different from that seen in 2D culture. However, the components of animal-derived materials, such as Matrigel, Collagen I, are complex and undefined[10]. This makes control difficult with these materials.

The self-assembling peptide RADA16-I (Ac-RADARADARADARADA-CONH₂), a simple model oligopeptide, is characterized by repeats of alternating ionic hydrophilic and hydrophobic amino acids[19]. RADA16-I can self-assemble to form stable nanofibers scaffolds in

the presence of monovalent cations or physiological media[26]. RADA16-I has been used to mimic the 3D microenvironment for various cell cultures [14, 19]. In present study, we applied RADA16-I as an ECM in 3D culture for the pancreatic cancer cell line-MIAPaCa-2 and compared this with Matrigel and Collagen I, and investigated the effects of these different materials on the malignant phenotype of MIAPaCa-2 cells.

Studies have demonstrated that RADA16-I supports the differentiation of rat pheochromocytoma cells[18], hepatocyte progenitor cells[29], and hippocampal neurons[30], the tubulogenesis of endothelial cell[31], and the attachment of some primary and transformed cell types[19]. Additionally, RADA16-I forms a more rigid hydrogel, which may provide a suitable scaffold for tumour cells[32]. In our study, the distribution and viabilities of MIAPaCa-2 cells cultured in RADA16-I were good.

Morphology and malignant phenotype significantly differed between these materials. MIAPaCa-2 cells in Collagen I showed a myofibroblast-like phenotype, while, on the other hand, MIAPaCa-2 cells in RADA16-I and Matrigel maintained a phenotype of multicellular spheroids. Epithelial-mesenchymal transition (EMT) has been found to contribute to many aspects of tumour biology and therapeutic resistance[33]. EMT is characterized by the loss of cell-to-cell adhesion, with the disintegration of tight adherents and gap junctions, and a phenotype change from an “epithelial” morphology to a motile, fibroblast-like morphology[34]. Thus, the myofibroblast-like phenotype of MIAPaCa-2 cells in Collagen I may be partially due to EMT, compared with RADA16-I and Matrigel.

Our results reveal that MIA PaCa-2 cells have differing proliferation potentials in different tumour-surrounding microenvironments: the pancreatic cancer cells in Matrigel proliferated prominently, due to the various growth factors; however, the cells in RADA16-I stopped proliferating gradually during the culture process, which may be due to the lack of animal-derived material. Matrigel is a mixture of components such as laminins, Collagen α , heparin sulfate proteoglycans, different growth factors and some undefined components[35]. Because Matrigel contains complex components, its mechanism for promoting tumour cell growth has not been comprehensively elucidated. Because RADA16-I consists of standard amino acids, without animal-derived factors, its scaffold is likely to be a promising alternative that creates a “clear” 3D nanostructure in the ECM. More studies using the RADA16-I peptide scaffold are under way to investigate different cell types [36, 37].

MIAPaCa-2 cells in RADA16-I clearly had reduced invasive potential in this study. The decline in proliferation and invasion of MIAPaCa-2 cells in RADA16-I is possibly due to the nanostructure of RADA16-I and the interactions between RADA16-I and MIAPaCa-2 cells. The study suggests that cells sense or respond to the nano-scale ECM, which may be regulated by the interaction between nano-structure and cells[38]. In RADA16-I, the different cell-surface components and mediators may play a crucial role in non-integrin mediated cell attachment to the RADA16-I[19]. The interactions change the way by which the integrins and the ECM interact through the receptor transduction pathways that regulate cell growth and invasion[39, 40], leading to the decline in proliferation and invasion by MIA PaCa-2 cells. However, the mechanisms behind these behaviours are not completely clear.

Furthermore, the results of tumour formation *in vivo* might be attributable to the suitable structure of Matrigel and Collagen I for MIA PaCa-2 cells during the process of transplantation of MIAPaCa-2 cells, and the presence of complex components, which include many growth factors

promoting the growth of pancreatic cancer cells *in vivo*. However, RADA16-I reduced the tumour weight and volume of MIA PaCa-2 cells *in vivo*, compared with Matrigel, Collagen I, and MIAPaCa-2 cells alone (control). We hypothesize that this may be due to the growth-inhibitory effect of RADA16-I on MIA PaCa-2 cells. A recent study showed that RADA16-I can suppress the formation of prostate cancer stem cell colonies *in vitro*. This study also suggested that the RADA16-I peptide scaffold could recreate cell-to-cell interactions, thus inhibiting cells, halting their proliferation, and suppressing tumour progression and metastasis[15].

5. Conclusions

In this study, we showed, for the first time, that the self-assembling peptide RADA16-I suppresses the malignant phenotype of pancreatic cancer cell line MIAPaCa-2 in three dimensional culture and *in vivo*. Our study also suggests that the microenvironment surrounding pancreatic cancer cells modifies their cellular behaviour. Research into the communication between cancer cells and the microenvironment will lead to the development of novel therapies. Furthermore, the self-assembling peptide RADA16-I may be a potential nanomaterial for pancreatic cancer research and treatment.

Conflicts of Interest

The authors report no conflicts of interest in this work.

References

- [1] K. Polyak, I. Haviv and I. G. Campbell, *Trends Genet* **25** (1), 30-38 (2009).
- [2] T. M. Desrochers, Y. Shamis, A. Alt-Holland, Y. Kudo, T. Takata, G. Wang, L. Jackson-Grusby and J. A. Garlick, *Epigenetics* **7** (1) (2012).
- [3] D. Hanahan and L. M. Coussens, *Cancer Cell* **21** (3), 309-322 (2012).
- [4] M. Erkan, G. Adler, M. V. Apte, M. G. Bachem, M. Buchholz, S. Detlefsen, I. Esposito, H. Friess, T. M. Gress, H. J. Habisch, R. F. Hwang, R. Jaster, J. Kleeff, G. Kloppel, C. Kordes, C. D. Logsdon, A. Masamune, C. W. Michalski, J. Oh, P. A. Phillips, M. Pinzani, C. Reiser-Erkan, H. Tsukamoto and J. Wilson, *Gut* **61** (2), 172-178 (2012).
- [5] M. Erkan, S. Hausmann, C. W. Michalski, A. A. Fingerle, M. Dobritz, J. Kleeff and H. Friess, *Nat Rev Gastroenterol Hepatol* (2012).
- [6] G. L. Beatty, E. G. Chiorean, M. P. Fishman, B. Saboury, U. R. Teitelbaum, W. Sun, R. D. Huhn, W. Song, D. Li, L. L. Sharp, D. A. Torigian, P. J. O'Dwyer, R. H. Vonderheide, *Science* **331** (6024), 1612-1616 (2011).
- [7] M. V. Apte and J. S. Wilson, *J Gastroenterol Hepatol* **27 Suppl 2**, 69-74 (2012).
- [8] E. Burdett, F. K. Kasper, A. G. Mikos and J. A. Ludwig, *Tissue Eng Part B Rev* **16** (3), 351-359 (2010).
- [9] K. M. Yamada and E. Cukierman, *Cell* **130** (4), 601-610 (2007).
- [10] S. Vukicevic, H. K. Kleinman, F. P. Luyten, A. B. Roberts, N. S. Roche and A. H. Reddi, *Exp Cell Res* **202** (1), 1-8 (1992).
- [11] X. Zhao, Y. Nagai, P. J. Reeves, P. Kiley, H. G. Khorana and S. Zhang, *Proc Natl Acad Sci U S A* **103** (47), 17707-17712 (2006).
- [12] S. Y. Fung, H. Yang and P. Chen, *Colloids Surf B Biointerfaces* **55** (2), 200-211 (2007).

- [13] R. G. Ellis-Behnke, Y. X. Liang, D. K. Tay, P. W. Kau, G. E. Schneider, S. Zhang, W. Wu, K. F. So, *Nanomedicine* **2** (4), 207-215 (2006).
- [14] K. Mi, G. Wang, Z. Liu, Z. Feng, B. Huang and X. Zhao, *Macromol Biosci* **9**(5), 437-443 (2009).
- [15] P. M. Ling, S. W. Cheung, D. K. Tay and R. G. Ellis-Behnke, *Cell Transplant* **20**(1), 127-131 (2011).
- [16] J. Yang, M. Yamato, K. Nishida, T. Ohki, M. Kanzaki, H. Sekine, T. Shimizu and T. Okano, *J Control Release* **116** (2), 193-203 (2006).
- [17] H. Meng, L. Chen, Z. Ye, S. Wang and X. Zhao, *J Biomed Mater Res B Appl Biomater* **89** (2), 379-391 (2009).
- [18] T. C. Holmes, S. de Lacalle, X. Su, G. Liu, A. Rich and S. Zhang, *Proc Natl Acad Sci U S A* **97**(12), 6728-6733 (2000).
- [19] S. Zhang, T. C. Holmes, C. M. DiPersio, R. O. Hynes, X. Su and A. Rich, *Biomaterials* **16** (18), 1385-1393 (1995).
- [20] J. L. Page, M. C. Johnson, K. M. Olsavsky, S. C. Strom, H. Zarbl and C. J. Omiecinski, *Toxicol Sci* **9** (2), 384-397 (2007).
- [21] C. H. Streuli, C. Schmidhauser, M. Kobrin, M. J. Bissell and R. Derynck, *J Cell Biol* **120** (1), 253-260 (1993).
- [22] J. M. Teare, R. Islam, R. Flanagan, S. Gallagher, M. G. Davies and C. Grabau, *Biotechniques* **22** (6), 1170-1174 (1997).
- [23] P. A. Kenny, G. Y. Lee, C. A. Myers, R. M. Neve, J. R. Semeiks, P. T. Spellman, K. Lorenz, E. H. Lee, M. H. Barcellos-Hoff, O. W. Petersen, J. W. Gray and M. J. Bissell, *Mol Oncol* **1**(1), 84-96 (2007).
- [24] A. Salic and T. J. Mitchison, *Proc Natl Acad Sci U S A* **105**(7), 2415-2420 (2008).
- [25] I. o. L. A. Research, C. o. L. Sciences and N. R. Council, *Guide for the Care and Use of Laboratory Animals*. (The National Academies Press, 1996).
- [26] H. Yokoi, T. Kinoshita and S. Zhang, *Proc Natl Acad Sci U S A* **102** (24), 8414-8419 (2005).
- [27] S. Dangi-Garimella, S. B. Krantz, M. R. Barron, M. A. Shields, M. J. Heiferman, P. J. Grippo, D. J. Bentrem and H. G. Munshi, *Cancer Res* **71** (3), 1019-1028 (2011).
- [28] Q. Liao, Y. Hu, Y. P. Zhao, T. Zhou and Q. Zhang, *Chin Med J (Engl)* **123** (14), 1871-1877 (2010).
- [29] C. E. Semino, J. R. Merok, G. G. Crane, G. Panagiotakos and S. Zhang, *Differentiation* **71** (4-5), 262-270 (2003).
- [30] C. E. Semino, J. Kasahara, Y. Hayashi and S. Zhang, *Tissue Eng* **10** (3-4), 643-655 (2004).
- [31] D. A. Narmoneva, O. Oni, A. L. Sieminski, S. Zhang, J. P. Gertler, R. D. Kamm, R. T. Lee, *Biomaterials* **26** (23), 4837-4846 (2005).
- [32] M. J. Paszek, N. Zahir, K. R. Johnson, J. N. Lakins, G. I. Rozenberg, A. Gefen, C. A. Reinhart-King, S. S. Margulies, M. Dembo, D. Boettiger, D. A. Hammer, V. M. Weaver, *Cancer Cell* **8** (3), 241-254 (2005).
- [33] K. Polyak and R. A. Weinberg, *Nat Rev Cancer* **9** (4), 265-273 (2009).
- [34] H. Peinado, D. Olmeda and A. Cano, *Nat Rev Cancer* **7** (6), 415-428 (2007).
- [35] H. K. Kleinman, M. L. McGarvey, L. A. Liotta, P. G. Robey, K. Tryggvason and G. R. Martin, *Biochemistry* **21** (24), 6188-6193 (1982).
- [36] P. C. Hsieh, M. E. Davis, J. Gannon, C. MacGillivray and R. T. Lee, *J Clin Invest* **116** (1), 237-248 (2006).
- [37] K. Hamada, M. Hirose, T. Yamashita and H. Ohgushi, *J Biomed Mater Res A* **84** (1), 128-136 (2008).
- [38] S. Heydarkhan-Hagvall, C. H. Choi, J. Dunn, S. Heydarkhan, K. Schenke-Layland, W. R. MacLellan, R. E. Beygui, *Cell Commun Adhes* **14** (5), 181-194 (2007).
- [39] Y. H. Soung, J. L. Clifford and J. Chung, *BMB Rep* **43** (5), 311-318 (2010).
- [40] D. Cox, M. Brennan and N. Moran, *Nat Rev Drug Discov* **9** (10), 804-820 (2010).

